# PCCP

Accepted Manuscript

Volume 1 | Number 1 | Jan 2013 | Pages 1–100

PCCP

Physical Chemistry Chemical Physics

www.rsc.org/pccp

ROYAL SOCIETY OF CHEMISTRY

ROYAL SOCIETY OF CHEMISTRY

www.rsc.org/pccp

Journal Name

ARTICLE

# Very rapid electronic relaxation process in a highly conjugated Zn(II)porphyrin–[26]hexaphyrin–Zn(II)porphyrin hybrid tape

Received 00th January 20xx,
Accepted 00th January 20xx

DOI: 10.1039/x0xx00000x

**www.rsc.org/**

Sangsu Lee,[a] Hirotaka Mori,[b] Taegon Lee,[c] Manho Lim,*[c] Atsuhiro Osuka*[b] and Dongho Kim*[a]

Excited-state energy relaxation processes of a Zn(II)porphyrin–[26]hexaphyrin–Zn(II)porphyrin triply linked hybrid tape, **FZn**, have been investigated by femtosecond transient absorption spectroscopy (TA), using a directly *meso*–*meso* linked hybrid trimer, **HZn**, as a reference compound. **FZn** has a very small $S_1$-$S_0$ energy gap through expansion of π-conjugation and a absorption band at 1897 nm corresponds to its lowest singlet excited-state as a consequence of enhanced transition dipole moment that lies parallel to the long molecular axis. In TA measurements, we observe a energy transfer process (0.4 ps) from Zn(II)porphyrin moiety to [26]hexaphyrin core in **HZn**. In contrast to **HZn**, biexponential decay with the time constants of 0.25 and 6.5 ps were observed in the decay profile of **FZn**. Detailed analysis of excitation wavelength, temperature and solvent dependent TA in **FZn** revealed that the electronic relaxation process (0.25 ps) from $S_1$ to $S_0$ is faster than the vibrational relaxation processes (5.9 ps) in the excited and ground state due to a very small $S_1$-$S_0$ energy gap through expansion of π-conjugation. Accordingly, we demonstrate that electronic deactivation overtakes vibrational relaxation processes in a highly conjugated **FZn**.

## Introduction

In light-responsive organic molecular systems, it has been important to understand their excited-state relaxation processes because the manipulation of excited-state dynamics often leads to the improvement in the performance of organic-dye-based molecular-level devices and functional soft materials.[1] Excited-state relaxation processes are largely governed by the electronic and vibrational relaxation processes. While the rate of vibrational relaxation processes is usually much faster than that of $S_1$-$S_0$ electronic relaxation process,[2] they may become competitive in well-conjugated systems. In our previous study on a series of triply linked Zn(II)porphyrin tapes, we demonstrated that the rate of $S_1$ state relaxation processes becomes saturated because of a competition between the electronic and vibrational relaxation processes as the $S_1$-$S_0$ energy gap decreases.[3] Additionally, in another series of porphyrin tapes with varying molecular length, we discovered that the excited-state energy relaxation processes of longer ones consisting of 4-6 units (5 ~ 13 ps) are slower than those of shorter ones containing 2-3 moieties (2.3 ~ 4.5 ps).[4] These results are seemingly contradictory to an expectation from the energy gap law because the $S_1$-$S_0$ energy gaps of the longer tapes are smaller than those of the shorter tapes.[5] From these previous results, we conjectured that the rate of $S_1$-$S_0$ electronic relaxation process can be faster than that of vibrational relaxation processes in well-conjugated molecules with sufficiently small $S_1$-$S_0$ energy gaps. However, our expectation in the fused porphyrin tapes has not yet been tested in full detail because Zn(II)porphyrin tapes used before are quite unstable due to facile oxidative decomposition in solution phase. Although this unusual excited-state relaxation process has been observed in small molecules, it is largely caused by structural dynamics in nπ* state and intramolecular charge transfer state.[6] However, we can assume that fused porphyrin tapes in the previous studies have similar structures in the excited and ground state because of their rigid structures.[7] Additionally, there were no evidence of intramolecular charge transfer dynamics in the previous fused porphyrin tapes. Therefore, we assume that excited-state relaxation processes in fused porphyrin tapes might be affected by sufficiently small $S_1$-$S_0$ energy gaps, excluding these structural and intramolecular charge transfer dynamics.

In this paper, we report the ultrafast excited-state decay dynamics of a triply linked Zn(II)porphyrin–[26]hexaphyrin–Zn(II)porphyrin hybrid tape, **FZn**, using a directly *meso*–*meso* linked hybrid trimer, **HZn**, as a reference compound (Fig. 1(a)). It should be noted that **FZn** is remarkably stable in solution under aerobic conditions,[8] differing from previously reported Zn(II)porphyrin tapes, which is suitable for the present study. Additionally, **FZn** exhibits a significantly red-shifted absorption band at 1897 nm as a reflection of effective red-shifting-ability by [26]hexaphyrin moiety that roughly corresponds to four

---

[a] Spectroscopy Laboratory for Functional π-Electronic Systems and Department of Chemistry, Yonsei University, Seoul 120-749, Korea
[b] Department of Chemistry and Graduate School of Science, Kyoto University, Sakyo-ku, Kyoto 606-8502, Japan
[c] Department of Chemistry and Chemistry Institute of Functional Materials, Pusan National University, Busan 609-735, Korea

† Electronic Supplementary Information (ESI) available: Experimental details, theoretical calculations, excitation wavelength, temperature and solvent dependent experiment results. See DOI: 10.1039/x0xx00000x

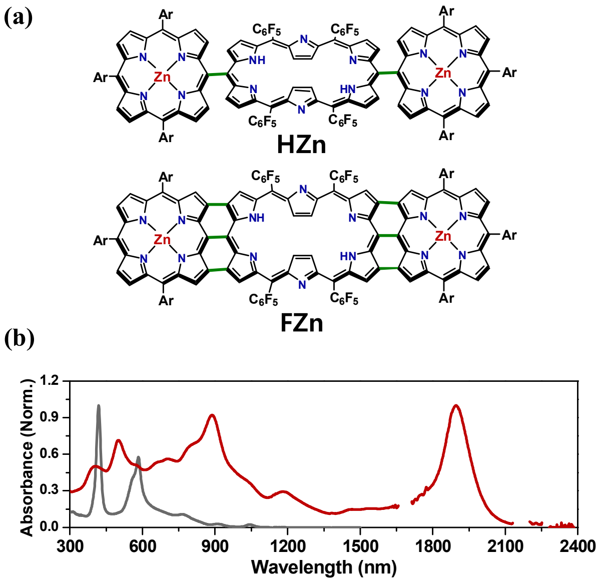

**Fig. 1** (a) Molecular structures of **HZn** and **FZn**; Ar = 3,5-di-tert-butylphenyl (b) Steady-state absorption spectra of **HZn** (gray) and **FZn** (red) in pure toluene and toluene containing 1% pyridine, respectively.

Zn(II)porphyrin units. In this regard, **FZn** is ideally suited for the investigation of excited-state relaxation processes affected by a very small $S_1$-$S_0$ energy gap.

## Results and discussion

The steady-state absorption spectra of **HZn** and **FZn** taken in pure toluene and toluene containing 1% pyridine at room temperature are shown in Fig. 1(b). To prevent possible aggregation of **FZn** through planar structure, we used toluene containing 1% pyridine as a solvent.[8] The absorption spectrum of **HZn** is nearly the sum of the absorption spectra of Zn(II)porphyrin and [26]hexaphyrin.[9] The absorption bands at 419 and 583 nm in **HZn** nearly match the B-bands of Zn(II)porphyrin and [26]hexaphyrin, respectively, indicating that electronic interaction between the Zn(II)porphyrin moieties and the [26]hexaphyrin core is negligible. In the case of **FZn**, the absorption spectrum exhibits a drastic red-shift as a consequence of expanded π-conjugation due to the completely fused planar structure (Fig. S1 in ESI). It has been established that the absorption band of Zn(II)porphyrin tapes in the near-infrared region originates from Q-band of a Zn(II)porphyrin monomer.[4] Although the Q-band in Zn(II)porphyrin monomer is only weakly allowed due to the cancellation of transition dipole moments according to Gouterman's four-orbital model,[10] a strong absorption band can be detected for Zn(II)porphyrin tapes in the near-infrared region due to an enhanced transition dipole moment that lies parallel to the long molecular axis. Therefore, it is reasonable to consider that the absorption band of **FZn** at 1897 nm corresponds to its lowest singlet excited-state. This is further supported by time-dependent density functional theory (TD-DFT) calculations (Table S1 and Fig. S2 in ESI). Also, the $S_0$-$S_1$ energy gap of **FZn** has been calculated to be 0.76 eV, which matches roughly the experimental value (0.65 eV). Therefore, we can confirm that **FZn** has a very small $S_1$-$S_0$ energy gap.

To examine the excited-state dynamics of **HZn** and **FZn**, we have measured the femtosecond transient absorption (TA) spectra of **HZn** and **FZn**. The white-light continuum (WLC) has an intrinsic group-velocity dispersion (GVD). When traveling through optically dense materials, the GVD of WLC increases to picoseconds.[11] To estimate accurate dynamics in fast time scale (< 1 ps), we have measured the chirpping of WLC from 450 to 1400 nm at each excitation wavelength.[12] In the case of **HZn**, we have employed the two excitation wavelengths to elucidate the interaction between Zn(II)porphyrin moieties (420 nm) and [26]hexaphyrin core (700 nm). Although the absorption band at 583 nm in **HZn** matches with the B-band of [26]hexaphyrin, the TA spectrum of **HZn** was measured upon photoexcitation at 700 nm because the peak at 583 nm in **HZn** is mixed with the B-state of [26]hexaphyrin and the Q-state of Zn(II)porphyrin. We observed a fast rise component (0.4 ps) and a relatively slow decay component (140 ps) upon photoexcitation of the Zn(II)porphyrin moiety at 420 nm, whereas only a slow decay component was observed when the [26]hexaphyrin core was directly excited at 700 nm (Figs. 2 and

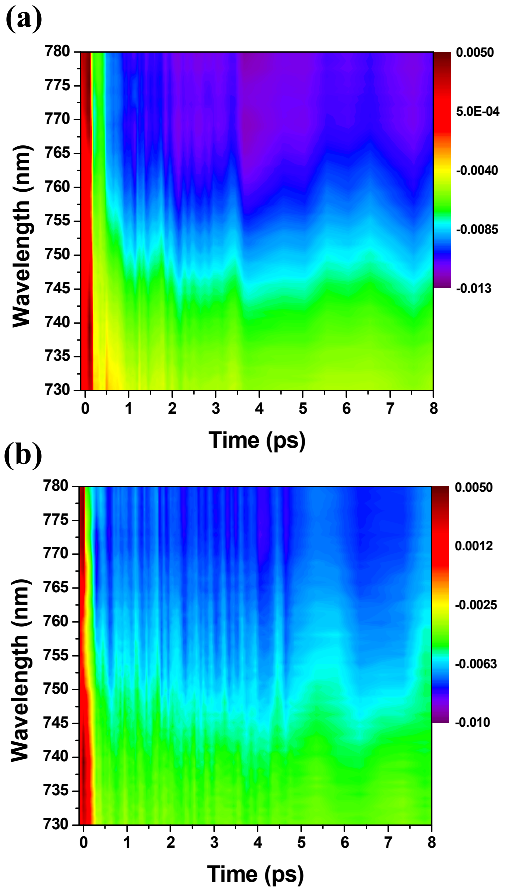

**Fig. 2** Two-dimensional TA contour map of **HZn** with photoexcitation at (a) 420 and (b) 700 nm in toluene. The color scale represents the transient absorption signals (ΔA).

S3 in ESI). To reveal the origin of rise (0.4 ps) and decay component (140 ps) in the TA decay profile of **HZn**, we have analysed the decay-associated spectra. Two separated components were observed with the time constants of 0.4 and 140 ps upon photoexcitation at 420 nm, which resemble the absorption spectra of Zn(II)porphyrin Q-band and [26]hexaphyrin B-band, respectively (Fig. S4 in ESI). Therefore, we can conclude that the 0.4 ps rise component which was only detected upon photoexcitation of the Zn(II)porphyrin moiety at 420 nm represents the energy transfer process from the Zn(II)porphyrin moiety to the [26]hexaphyrin core and the 140 ps decay component corresponds to the singlet excited-state lifetime of the [26]hexaphyrin core in **HZn**.[8] In fact, fast decay component at Zn(II)porphyrin bleaching in the TA spectrum of **HZn**, which is coincident with fast rise component (0.4 ps), should be observed for an accurate analysis of energy transfer process from the Zn(II)porphyrin moiety to [26]hexaphyrin core. However, we cannot extract pure Zn(II)porphyrin state from the TA spectrum of **HZn** because Zn(II)porphyrin state is mixed with [26]hexaphyrin state in the TA spectrum of **HZn**. Nevertheless, we can confirm the energy transfer process from the Zn(II)porphyrin moiety to the [26]hexaphyrin core through the analysis of excitation energy dependent TA decay profiles and decay-associate spectra. Although **HZn** shows a relatively weak interaction between Zn(II)porphyrin and [26]hexaphyrin moieties in the steady-state absorption spectrum due to its orthogonal structure through the *meso-meso* single bond linkage (Fig. S1 in ESI), we observed a signature of ultrafast energy transfer from the Zn(II)porphyrin moiety to the [26]hexaphyrin core because the distance between the Zn(II)porphyrin moiety and the [26]hexaphyrin core is very short.

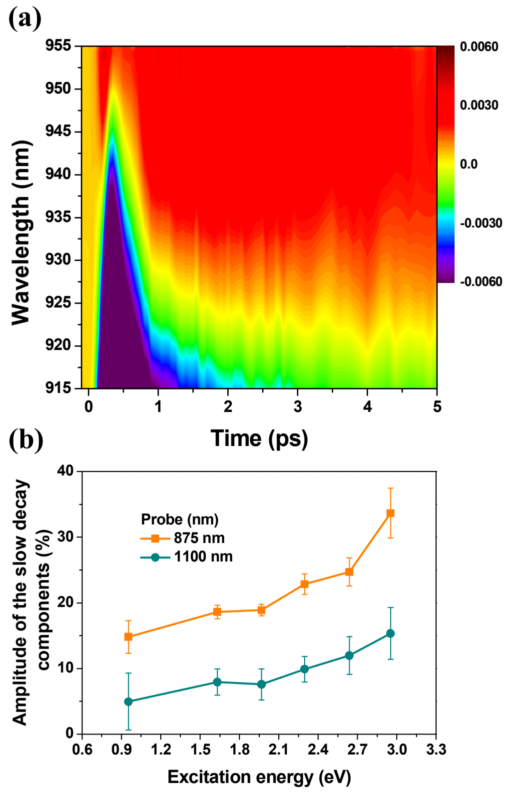

**Fig. 3** (a) Two-dimensional TA contour map of **FZn** with photoexcitation at 630 nm in toluene containing 1% pyridine. The color scale represents the transient absorption signals (ΔA). Thus, the crossing points (ΔA=0) between excited-state absorption and ground-state bleaching spectra are represented by yellow color. (b) Amplitude of the slow decay components in **FZn** probed at 875 and 1100 nm by changing the photoexcitation wavelength from 420 to 1300 nm.

On the other hand, we could not observe such fast rise dynamics originated from energy transfer process upon photoexcitation of the Zn(II)porphyrin moiety at 420 nm in **FZn** (Figs. S5 and S6 in ESI). Instead, ultrafast decay components of 0.25 and 5.9 ps were observed in the TA decay profiles of **FZn**. This result implies that **FZn** can be regarded as a single chromophore system due to fully expanded π-conjugation network.[9b] Therefore, we can consider only the electronic and vibrational relaxation processes by the excited-state dynamics of **FZn** excluding energy transfer process from the Zn(II)porphyrin moiety to the [26]hexaphyrin core.

To figure out the origin of 0.25 and 5.9 ps decay components in **FZn**, we have measured the excitation wavelength dependent TA spectra by systematically changing the pump wavelength from 420 to 1300 nm. Although the instrument response function of our TA set-up can be changed at each excitation wavelength, we can confirm definite biexponential decay profiles in **FZn** at all the excitation wavelengths because the fast decay component (0.25 ps) is nearly 25 times faster than the slow decay component (5.9 ps). Additionally, it is should be noted that the fast decay components in **FZn** showed no significant differences because the limited time resolution of our TA setup (~150 fs) made it almost impossible to differentiate small changes in the fast time components at all excitation wavelengths. Although we could detect the decay components of 0.25 and 5.9 ps at all excitation wavelengths (Fig. S6 in ESI), the two unique features were observed. First, the edge of the excited-state absorption spectra in the near-infrared region was blue-shifted from 950 to 920 nm regardless of the pump wavelength as the delay time increases (Figs. 3(a) and S7 in ESI). Upon initial excitation, the excited-state absorption is dominated by transition from the vibrationally excited-state manifolds in the electronically excited-state to higher excited-states. After the vibrational relaxation to the vibrationally ground but electronically excited-state, the excited-state absorption spectra move to shorter wavelength.[13] Thus, this blue-shift is likely to represent the vibrational relaxation processes in the electronically excited-state. These vibrational relaxation processes in porphyrin complexes were observed on the time scale of about 10 ps.[14] Therefore, we can assume that the excited-state relaxation dynamics of **FZn** is affected by the vibrational relaxation processes. The rate of these spectral evolutions in the edge of the excited-state absorption corresponding to the vibrational relaxation processes can be presented by the time trace of crossing points (ΔA=0) between the excited-state absorption and ground-state bleaching bands (Fig. S8 in ESI). Also, the amplitude of slow decay components (5.9 ps) in the TA decay profiles gradually decreases as the excitation energy decreases (Fig. 3(b) and Table S3 in ESI). In general it is

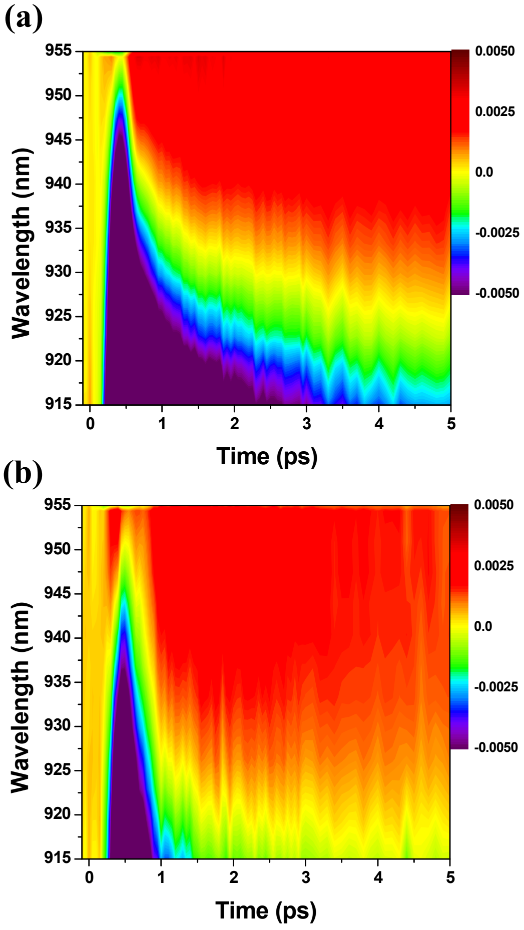

**Fig. 4** Two-dimensional TA contour map of **FZn** in 2-meTHF with photoexcitation at 630 nm at (a) 77 and (b) 297 K. The color scale represents the transient absorption signals (ΔA). Thus, the crossing points (ΔA=0) between excited-state absorption and ground-state bleaching spectra are represented by yellow color.

expected that the amplitude of faster decay component in the decay profile should be reduced in the decay dynamics as the excitation energy decreases because the faster decay process can be assigned as the relaxation dynamics occurring in the higher excited-state, i.e internal conversion (IC), vibrational relaxation. However, we observed the exactly opposite tendency in our measurements.

In order to elucidate the origin of the two decay components in **FZn**, we have measured the TA spectra at various temperatures in 2-methyltetrahydrofuran (2-meTHF). Prior to TA measurements, we have measured the temperature-dependent steady-state absorption spectra of **FZn** (Fig. S9 in ESI). The overall spectra became slightly red-shifted and sharper as the temperature was lowered from 297 to 77 K. From the negligible variation observed in the peak position of **FZn**, we can ensure that **FZn** has no structural flexibility because of its rigid molecular structure arising from the fused geometry. Therefore, we can analyse the temperature-dependent TA spectra by excluding the structural dynamics. The TA results obtained at 77 and 297 K showed some differences in the spectral changes and decay profiles. Although the TA spectra at 77 and 297 K show commonly the blue-shift in the excited-state absorption band, the dynamics of spectral evolutions is different depending on the temperature (Figs. 4, S10 and S11 in ESI). The rate of spectral evolutions (0.9 ps) at 77 K is slower than that (0.4 ps) at 297 K. Because the spectral evolution is contributed by the vibrational relaxation processes, we can assume that the vibrational relaxation processes of **FZn** are changed by temperature. Additionally, the slow decay component (5.2 ps) at 77 K is slightly longer than that (4.4 ps) at 297 K**,** but the fast decay components (0.25 ps) were insensitive to the temperature (Fig. S12 in ESI). Therefore, we can conclude that the fast decay component of 0.25 ps is mainly attributed to the electronic transition and the slow decay components to the vibrational relaxation processes of **FZn**, respectively. This analysis leads to an unusual situation that the vibrational relaxation is slower than the electronic relaxation in **FZn**, which is opposite to the generally expected excited-state dynamics in organic molecular systems with absence of structural dynamics and charge transfer state.

To reveal the reason why the rate of vibrational relaxation processes is slower than that of electronic relaxation ones in **FZn**, we further discuss the origin of vibrational relaxation processes. In general, there are two different factors contributing to the vibrational relaxation processes ($k_{\mathrm{vib}}$), i.e. intramolecular vibrational relaxation (IVR) and intermolecular vibrational energy transfer process (VET). Both processes are directly related to the rate of vibrational relaxation by equation 1.[15]

$$k_{vib} = \frac{1}{\tau_{vib}} = k_{IVR} + k_{VET} \qquad (1)$$

The VET process ($k_{VET}$) occurs via coupling between the vibrational states and the surrounding medium, which is usually slower than the IVR process ($k_{IVR}$).[16] The efficiency of the VET process is governed by the vibrational frequency ($\omega_n$) as well as the spectral density of the fluctuating external solvent force ($\delta F_n^e$) (equation 2).[17]

$$k_{VET} = \frac{1}{\tau_{VET}} = \frac{1}{\mu_n k_B T}\int_0^\infty \langle \delta F_n^e(t)\delta F_n^e(0)\rangle \cos \omega_n t \, dt \qquad (2)$$

The latter depends on the properties of the mode specific solute–solvent interactions, which can be estimated from an overlap between the solute and solvent absorption spectra. In the absorption spectra of **FZn** and pure toluene, we can find an overlap between the electronic states of **FZn** and the vibrational modes of pure toluene (Fig. S13(a) in ESI). Specifically, the first overtone of the C—H stretching mode of toluene (~1600 nm) largely overlaps with the excited-state of **FZn**.[18] Therefore, we can assume that the slow decay component in the TA decay profiles of **FZn** corresponding to the vibrational relaxation processes is affected by the VET process in the excited-state of **FZn**.

To confirm the VET process from the excited-state manifolds of **FZn** to the C—H stretching mode of toluene, we have measured the TA decay profiles in toluene-$d_8$. Because all hydrogen atoms in toluene are substituted by deuterium

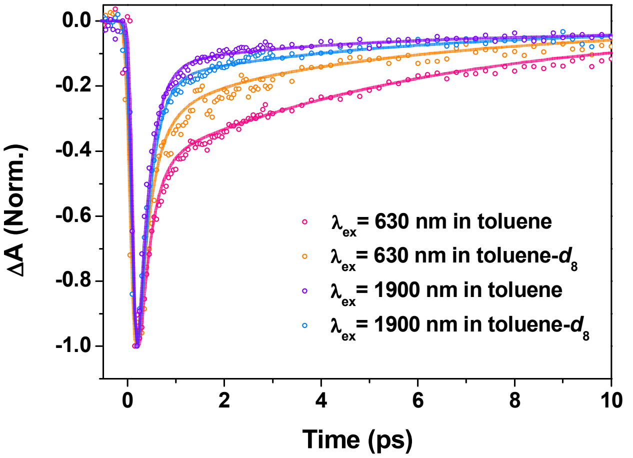

**Fig. 5** Normalized TA decay profiles of **FZn** measured in toluene containing 1% pyridine; green: pump 630 nm; red: pump 1900 nm, and measured in toluene-$d_8$ containing 1% pyridine; blue: pump 630 nm; orange: pump 1900 nm.

atoms in in toluene-$d_8$, we cannot observe the C—H stretching mode in the absorption spectrum of toluene-$d_8$. Instead, the first overtone of C—D stretching mode of toluene-$d_8$ (~2300 nm) was observed,[18] which is well separated from the absorption spectrum of **FZn** (Fig. S13(b) in ESI). Upon photoexcitation of **FZn** at 630 nm in toluene and toluene-$d_8$, we could observe biexponential decays in the TA decay profiles. However, the slow decay component (6.5 ps) in toluene-$d_8$ became slightly longer than that (5.9 ps) in toluene**,** but the fast decay components (0.25 ps) were insensitive to the solvent (Figs. 5 and S14 in ESI). Because the excitation energy (630 nm) is higher than the energy of the first overtone of the C—H stretching mode of toluene (~1600 nm), the VET process between the excited-state manifolds of **FZn** and the C—H stretching mode of toluene is possible. However, the VET process is absent in toluene-$d_8$ because there are no vibrational modes of toluene-$d_8$, which are overlapped with the excited-state manifolds of **FZn**. Therefore, this difference in the slow decay components of **FZn** depending on the solvent can be explained by the difference in the efficiency of the VET process between the excited-state manifolds of **FZn** and the C—H stretching modes of toluene. On the other hand, upon photoexcitation of the lowest singlet excited-state at 1900 nm, the same biexponential decays with the time constants of 0.25 and 6.5 ps were observed in toluene and toluene-$d_8$. Because the energy of the first overtone of C-H stretching mode of toluene (~1600 nm) is higher than the excitation energy (1900 nm), the VET process between the excited-state manifolds of **FZn** and the C—H stretching mode of toluene can be neglected. Therefore, this result further support the VET process between excited-state manifolds of **FZn** and the C—H stretching mode of toluene, which indicate that the VET process contributes to the vibrational relaxation processes of **FZn**.

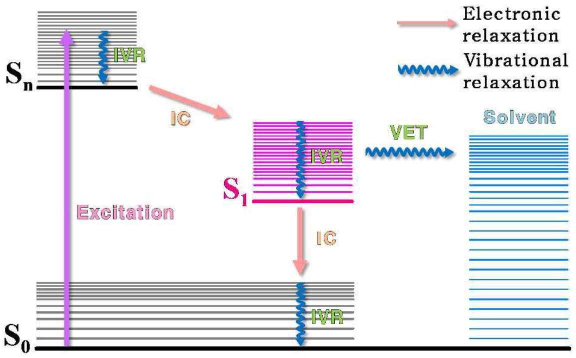

**Scheme 1.** Schematic diagram of the energy relaxation dynamics in **FZn**.

Moreover, we can assume that the vibrational relaxation processes of **FZn** are also affected by the IVR processes. In the excitation wavelength dependent TA spectra, we discovered that the amplitude of the slow decay component (5.9 ps) gradually decreased as the excitation energy decreased. If the vibrational relaxation process only contains the VET process between the excited-state manifolds of **FZn** and the C—H stretching mode of toluene, there should be no change in the amplitude of slow decay component upon changing the photoexcitation energy from 420 to 1300 nm because these excitation energies are higher than the first overtone of the C—H stretching mode of toluene (~1600 nm).

Additionally, in the case of TA decay profiles upon photoexcitation at 1900 nm corresponding to the lowest excited state of **FZn**, we cannot obtain single exponential decay profile. Therefore, the vibrational relaxation process of **FZn** is contributed by a combination of the excited and ground state vibrational relaxation processes. These excited-state relaxation processes of **FZn** are presented in Scheme 1. Upon initial excitation, the excited-state relaxation processes through IC and IVR processes occur from higher excited-state to the lowest excited-state manifolds. After the relaxation, IVR, VET and IC processes are possible in the $S_1$ state. Therefore, we can conclude that the energy relaxation processes in **FZn** are contributed by the interplay between the different vibrational relaxation processes in the excited and ground states.

## Conclusions

In this work, we report the unusual energy relaxation behaviors of the excited Zn(II)porphyrin–[26]hexaphyrin–Zn(II)porphyrin hybrid tape **FZn**. Namely, the electronic relaxation process (0.25 ps) from $S_1$ to $S_0$ is faster than the vibrational relaxation processes (5.9 ps) in the excited and ground state because of its highly conjugated nature. Moreover, the vibrational relaxation processes of **FZn** have been shown to be contributed by the IVR process in the excited and ground state, and the VET process between the first overtone of toluene C—H stretch and the excited-state manifolds of **FZn**. While the energy relaxation dynamics of large chromophores absorbing in a broad wavelength range have been reported in previous studies, this is the first study, to the best our knowledge, to demonstrate that the electronic deactivation overtakes the vibrational relaxation processes in the energy relaxation processes from the initially excited vibronic state manifolds in highly conjugated molecular systems just like our **FZn** system. In other words, although we cannot separate the IVR and VET dynamics, we unveil the origin of the slow dynamics in molecular arrays with an extremely small $S_1$-$S_0$ energy gap.

## Acknowledgements

The work at Yonsei University was supported by Global Research Laboratory (2013K1A1A2A02050183) through the National Research Foundation of Korea (NRF) funded by the Ministry of Science, ICT (Information and Communication Technologies) and Future Planning. The work at Kyoto was supported by JSPS KAKENHI Grant Nos. 25220802 and 25620031. H.M. acknowledges JSPS Fellowship for Young Scientists. The work at Pusan National University was supported by National Research Foundation of Korea (NRF) grants funded by the Korea government (MEST) (NRF-2014R1A2A2A01002456, NRF-2014R1A4A1001690).

## Notes and references

1 (a) J. M. Tour, *Chem. Rev.*, 1996, **96**, 537; (b) P. F. H. Schwab, M. D. Levin and J. Michl, *Chem. Rev.*, 1999, **99**, 1863; (c) J. Cornil, D. Beljonne, J.-P. Calbert and J.-L. Brédas, *Adv. Mater.*, 2001, **13**, 1053.
2 N. J. Turro, V. Ramamurthy and J. C. Scaiano, *Principles of Molecular Photochemistry: An Introduction*, University Science Books, Sausalito, CA, 2009
3 P. Kim, T. Ikeda, J. M. Lim, J. Park, M. Lim, N. Aratani, A. Osuka and D. Kim, *Chem. Commun.*, 2011, **47**, 4433
4 H. S. Cho, D. H. Jeong, S. Cho, D. Kim, Y. Matsuzaki, K. Tanaka, A. Tsuda and A. Osuka, *J. Am. Chem. Soc.*, 2002, **124**, 14642.
5 R. Englman and J. Jortner, *Mol. Phys.*, 1970, **18**, 145.
6 (a) T. Fujino and T. Tahara, *J. Phys. Chem. A*, 2000, **104**, 4203; (b) F. Frei, A. Rondi, D. Espa, M. L. Mercuri, L. Pilia, A. Serpe, A. Odeh, F. Van Mourik, M. Chergui, T. Feurer, P. Deplano, A. Vlček Jr. and A. Cannizzo, *Dalton Trans*., 2014, **43**, 17666.
7 M. J. Frampton, G. Accorsi, N. Armaroli, J. E. Rogers, P. A. Fleitz, K. J. McEwan and H. L. Anderson, *Org. Biomol. Chem.*, 2007, **5**, 1056.
8 H. Mori, T. Tanaka, S. Lee, J. M. Lim, D. Kim and A. Osuka, *J. Am. Chem. Soc.*, 2015, **137**, 2097.
9 (a) W.-Y. Cha, J. M. Lim, M.-C. Yoon, Y. M. Sung, B. S. Lee, S. Katsumata, M. Suzuki, H. Mori, Y. Ikawa, H. Furuta, A. Osuka and D. Kim, *Chem.–Eur. J.*, 2012, **18**, 15838; (b) S. Lee, H. Chung, S. Tokuji, H. Yorimitsu, A. Osuka and D. Kim, *Chem. Commun.*, 2014, **50**, 2947.
10 M. Gouterman, *J. Mol. Spectrosc.*, 1961, **6**, 138.
11 R. Berera, R. van Grondelle and J. T. M. Kennis, *Photosynth. Res.*, 2009, **101**, 105.
12 A. Maciejewski, R. Naskrecki, M. Lorenc, M. Ziolek, J. Karolczak, J. Kubicki, M. Matysiak and M. Szymanski, *J. Mol. Struct.*, 2000, **555**, 1.
13 D. A. Roberts, B. Fückel, R. G. C. R. Clady, Y. Y. Cheng, M. J. Crossley and T. W. Schmidt, *J. Phys. Chem. A*, 2012, **116**, 7898.
14 (a) O. Bilsel, S. N. Milan, G. S. Girolami, K. S. Suslick and D. Holten, *J. Phys. Chem.*, 1993, **97**, 7216; (b) O. Bilsel, J. Rodriguez and D. Holten, *J. Phys. Chem.*, 1990, **94**, 3508.
15 H. S. Yoo, M. J. DeWitt and B. H. Pate, *J. Phys. Chem. A*, 2004, **108**, 1365.
16 J. Assmann, R. v. Benten, A. Charvat, and B. Abel, *J. Phys. Chem. A,* 2003, **107**, 5291.
17 G. Käb, C. Schröder and D. Schwarzer, *Phys. Chem. Chem. Phys.*, 2002, **4**, 271.
18 H. G. Kjaergaard, D. M. Turnbull and B. R. Henry, *J. Phys. Chem. A*, 1997, **101**, 2589.